Fundamental mechanisms in chemical interaction between C-bonded refractories and steel"

Filippo Cirilli, Antonello Di Donato – Centro Sviluppo Materiali SpA - Italy
Pascal Dupel, Philippe Guillo – Vesuvius International - USA

Abstract

A set of experimental trials (corrosion tests) has been carried out aimed at elucidating the fundamental mechanisms in steel-refractory interaction.

The corrosion tests consist of keeping in contact molten steel with a rotating refractory rod. Steel has been sampled at regular times and then analysed.
Sections of the rods have been observed by using optical and electronic microscope, (OM and SEM).

Four different refractory systems have been investigated :
MgO-C
Al_2O_3-C
Al_2O_3-SiO2-C and
ZrO2-C

Taking into account of:

-   refractory carbon dissolution in the steel;
-   steel penetration inside the refractory;
-   reactions between refractory components forming new oxides and gaseous species;
-   interactions between steel components and chemical species coming from the refractory.

occurring during the tests, a mathematical model of the steel refractory interaction has been developed.
The model reproduces in a qualitative and quantitative way the experimental results, allows the choice of proper refractory and provides criteria for design new refractories for specific use.

1. Introduction

The production of super clean steel has put in clear evidence the role of the refractory in determining the level of internal pollution of the steel.
The decrease of the internal pollution caused by the chemical interaction between liquid steel and refractory has then become mandatory for the improvement of the product quality.
Decreasing the interaction between steel and refractory results in improving steel cleanliness.

In order to elucidate the importance of different phenomena operating in refractory corrosion caused by liquid steel, a proper experimental activity has been set up aiming at evidencing the role of each basic phenomenon on the extent of the global corrosion.

On the basis of the experimental activity a model for simulating and predicting the evolution of refractory and steel compositions has been developed.

The model permits the choice of proper refractory and provides criteria for designing new refractory for specific use.

For clarifying the kinetics laws governing the basic phenomena and controlling steps of the mechanisms occurring during refractory and liquid steel interaction, corrosion tests and thermogravimetric measurements have been performed under strictly controlled conditions.

2. Experimental activity

2.1. Materials

The experiments were carried out on refractory samples purposely prepared belonging to the systems reported in Table 1, with different characteristics, and synthetic metallic iron alloys of different compositions (Table 2).

Four different refractory systems have been investigated; their main characteristics are reported in Table 1.

2.2. Apparatus

A programmable electric furnace with graphite electrodes has been used for the corrosion tests.
The synthetic steel is prepared in an alumina crucible by melting a mixture of ARMCO iron and appropriate amounts of aluminium, silicon and manganese to obtain the target composition. To prevent oxidation the atmosphere was held at controlled oxygen potential.
For all the trials an average amount of 300-350 g of steel is used.

A rod of refractory material is put inside the molten steel. The corrosion test starts when the rod is immersed and lasts for about 1-2 hours at temperature held fixed at 1600°C ± 1.
The test can be made both with the rod under static and rotating conditions.
During the tests samples of steel are taken and chemically analysed.

Thermogravimetric tests are performed in a sealed thermobalance consisting of an electric furnace with a balance continuously measuring the sample mass in static conditions.
Thermogravimetric tests have been carried out with refractory samples alone to study the internal reactions among refractory components avoiding the influence of liquid steel.
The experiments are carried out in Argon atmosphere (Figure 2).
A mass spectrometer is connected to the thermobalance to measure the gas composition inside the furnace.
The experiments are carried out at 1600°C ± 1.

Chemical analysis, electron microscope with micro chemical analysis (SEM EDS) and X ray diffraction (XRD) have been used to measure the chemical modifications of the steel and refractory.

3. Results

The experimental tests permitted to identify the main fundamental mechanisms and their controlling steps.

The phenomena investigated and evidenced in the corrosion tests have been:
- carbon dissolution
- steel penetration
- reactions in the refractory
- formation of new phase in the metal

3.1. Carbon dissolution in the steel

The solid carbon in the refractory dissolves in the steel. As a consequence the carbon concentration in steel inside the crucible increases during the corrosion tests.

The dissolution rate of carbon is affected by possible variations of the refractory structure in the Interface zone during the test, due to reactions among the different oxides forming the refractory bulk, and deposition on the refractory surface of oxides formed inside the steel.
To avoid the influence of such phenomena on the carbon dissolution, experiments with technologically pure ZrO_2-C, Al_2O_3-C and MgO-C, interacting with steel at low concentration of dissolved elements, have been carried out. In these experiments no significant variation of the refractory in the Interface occurs.

The carbon dissolution rate results controlled by the rate of carbon diffusion inside the steel, [1, 2, 3]. Having assumed that at the refractory surface carbon saturation in steel occurs carbon dissolution rate is proportional to the carbon concentration gradient between the saturation value and the steel bulk value.

Figure 3, comparing experimental and computed mass of dissolved carbon, shows the adequacy of the above assumed dissolution rate.

The effect of fluid dynamic conditions has been experimentally verified performing corrosion tests at different angular speeds. Figure 4 shows the different rates of carbon dissolution experimentally measured for zirconia graphite refractory as a function of two rod angular speeds (30 and 60 revolutions per minute).

3.2. Steel penetration

At the end of each test the surface of the refractory, observed with SEM, appears modified (interface zone), as consequence of the interaction with steel, for different depth. The thickness and characteristics of the interface depend on refractory, metal, and test conditions.

In general the interface shows the presence of penetrated steel. The steel penetration is a consequence of the dissolution of solid carbon and variation of refractory structure.
Figure 5 shows SEM images of a ZrO_2-C refractory where the voids left by the carbon previously present are filled by steel penetrated inside the refractory.
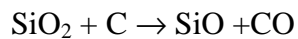

3.3. Reactions in the refractory

Reactions in the refractory can result in the formation of new phases changing the global structure of Interface, can be formed through different mechanisms.

Special attention was paid to study the gas forming reactions inside the refractory and the reactions among these gases with steel components.

Solid graphite reacts with refractory oxides forming new solid phase and/or gaseous compounds.
Examples of such reactions are [4, 5, 6, 7, 8]:

$$SiO_2 + C \rightarrow SiO + CO$$
$$MgO + C \rightarrow Mg + CO$$
$$ZrO_2 + 3C \rightarrow ZrC + 2CO$$
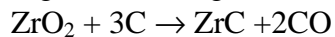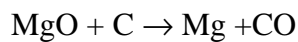
All these reaction products are gaseous except ZrC.
The refractory characteristics, like porosity [5] and gas permeability [11] affect the gas evolution rate and, as a consequence, reaction rates. Reference [5] reports that the diffusion rate of gases through the interface zone is the controlling step of the gas forming reactions.
During interaction between refractory and steel, gas permeability of the interface changes due to the deposition of oxides formed inside the steel.
Thermogravimetric experiments under inert Argon atmosphere, coupled with gas analysis, permitted to estimate the rate of the gas forming reactions as a function of the refractory porosity through the refractory mass variation.

As an example, Figure 6 shows the mass losses, recorded in thermogravimetric experiments carried out at 1600 °C under argon atmosphere, of refractory material (Al_2O_3-SiO_2-C), purposely prepared with two different porosities (10% and 14% by volume)

3.4. Formation of new oxides inside the steel

The gases formed inside the refractory can react with steel components [5].
For example, SiO and CO react, , with dissolved Aluminium forming Al_2O_3 and increasing the dissolved silicon and carbon. concentration, according to the following reaction:

$$3SiO + 2\underline{Al} \rightarrow 3\underline{Si} + Al_2O_3$$

$3CO + 2\underline{Al} \rightarrow 3\underline{C} + Al_2O_3$
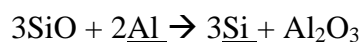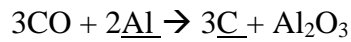
Increase of Si concentration in the steel caused by the above reaction has been observed experimentally.

Figure 7 shows an example of Si concentration increase together with dissolved Al concentration decrease measured in a corrosion test carried out with Al_2O_3-SiO_2-C refractory in the synthetic steel of Table 2.

The oxides formed by these reaction can deposit on the refractory surface forming new phases as shown in Figures 8 and 9.

Coupling the thermogravimetric and corrosion experiments can derive a global rate of the reaction producing new oxide inside the steel and provide the basic information for the mathematical modelling.

Model development

The above results have been used to develop a mathematical model quantitatively describing the main phenomena occurring during refractory/steel interaction.

In the model, the rate of carbon diffusion, reactions among refractory oxides and the formation of new oxides inside the steel are considered.

The parameters used in the model are physicol-chemical in nature: diffusion coefficients in bulk steel, effective diffusion coefficients through the interface

The effective diffusion coefficients being not available in literature have been estimated and adjusted comparing computed and experimental results.

The model permits to calculate the evolution in time of:

- rate of refractory mass loss as a consequence of the carbon dissolution and reaction between oxide and graphite
- depth of interface
- time evolution of steel composition

Figures 10, 11 and 12 show comparisons between experimental and computed results.

Referring to the system ZrO_2 -C in contact with synthetic steel, Figure 10 shows the time evolution of carbon concentration in the metal for two different refractory rod angular speeds.

Figure 11 shows the time evolution of concentration of the synthetic steel components, when interacting with a Al_2O_3-SiO_2-C refractory rod rotating at 30 revolution per minute.

Figure 12 shows the penetration depth of steel in two Al_2O_3-C refractory rod at two different solid carbon content rotating at 30 revolution per minute in contact with synthetic steel.

4. Conclusions

The fundamental mechanisms and laws governing the phenomena occurring in refractory and steel interaction have been identified by laboratory experiments using corrosion tests and thermogravimetric measurements.

A mathematical model based on the experimental results has been implemented, which permits the quantitative prediction of :

- rate of refractory mass loss as a consequence of the carbon dissolution and reaction between oxide and graphite
- depth of interface
- time evolution of steel composition

The model permits the choice of proper refractory and provides criteria for designing new refractory for specific use also.

References

1. R. B. Bird, W. E. Stewart, E. N. Lightfoot, Transport Phenomena, chapter 2 and 16 - Wiley International Edition, (1960)

2. F. Oeters. Metallurgy of steelmaking. Springer Verlag Berlin (1989)

3. A. R. Cooper, W. D. Kingery, Dissolution in Ceramic systems: Molecular diffusion, natural convection, and forced convection studies of sapphire dissolution in calcium aluminium silicate - Journal of the American Ceramic Society, 47, 1, 37-43, (1964)

4. Mukai - a mechanism for the local corrosion of immersion nozzles - ISIJ International, 29, 6, 469-476, (1989)

5. K. Sasai, Y. Mizukami - Reaction rate between alumina graphite immersion nozzle and low carbon steel - ISIJ International, 35, 1, 26-33,(1995)

6. K. L. Komarek et al, Reactions between refractory oxides and graphite - Journal of the Electrochemical Society, 110, 7, 783-791, (1963)

7. V. Brabie, Mechanism of reaction between refractory materials and Al deoxidised molten steel - ISIJ International , 36, s109-s112, (1996)

8. V. Brabie, The reaction of carbon monoxide in aluminium deoxidised molten steel - Scandinavian Journal of metallurgy, 25; 148-160, (1996)

9. Y. Gao, K. Sorimachi, formation of clogging materials in an immersed nozzle during continuos casting of titanium stabilised stainless steel, ISIJ International, 33, 2, 291-297, (1993)

10. Y. Fukuda, Y. Ueshima, S. Mizoguchi, Mechanism of alumina deposition on alumina graphite immersion nozzle in continuos caster, ISIJ International, 32, 1, 291-297, (1992)

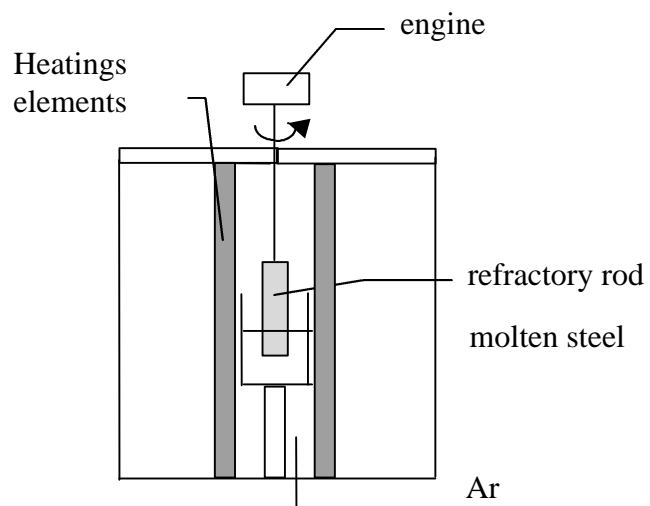11. G. Routschka et al, Gas permeability of refractories at elevated temperatures,

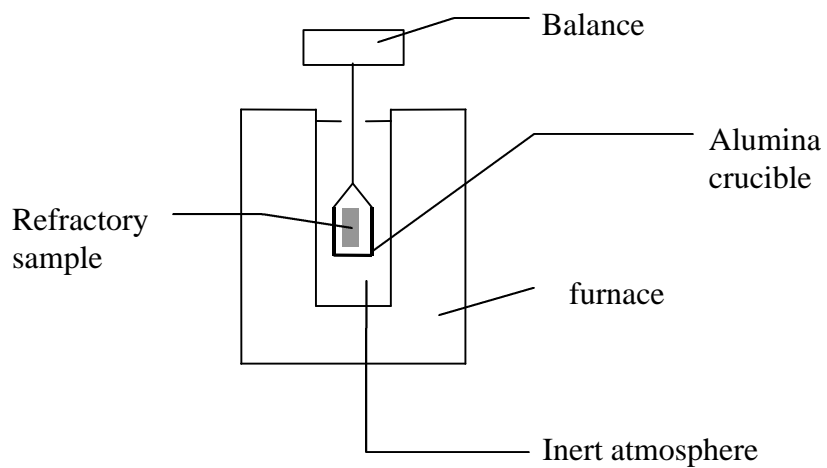**Figure 1. Experimental apparatus for corrosion tests.**

Figure 2. Experimental apparatus for thermogravimetric tests
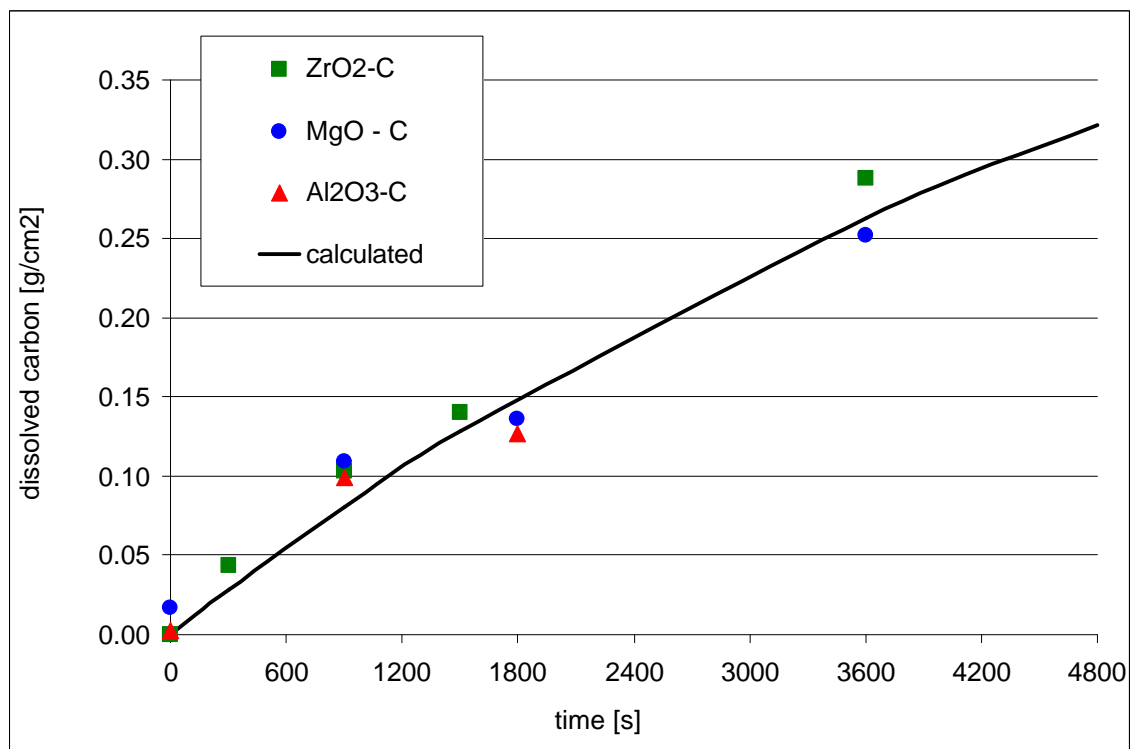
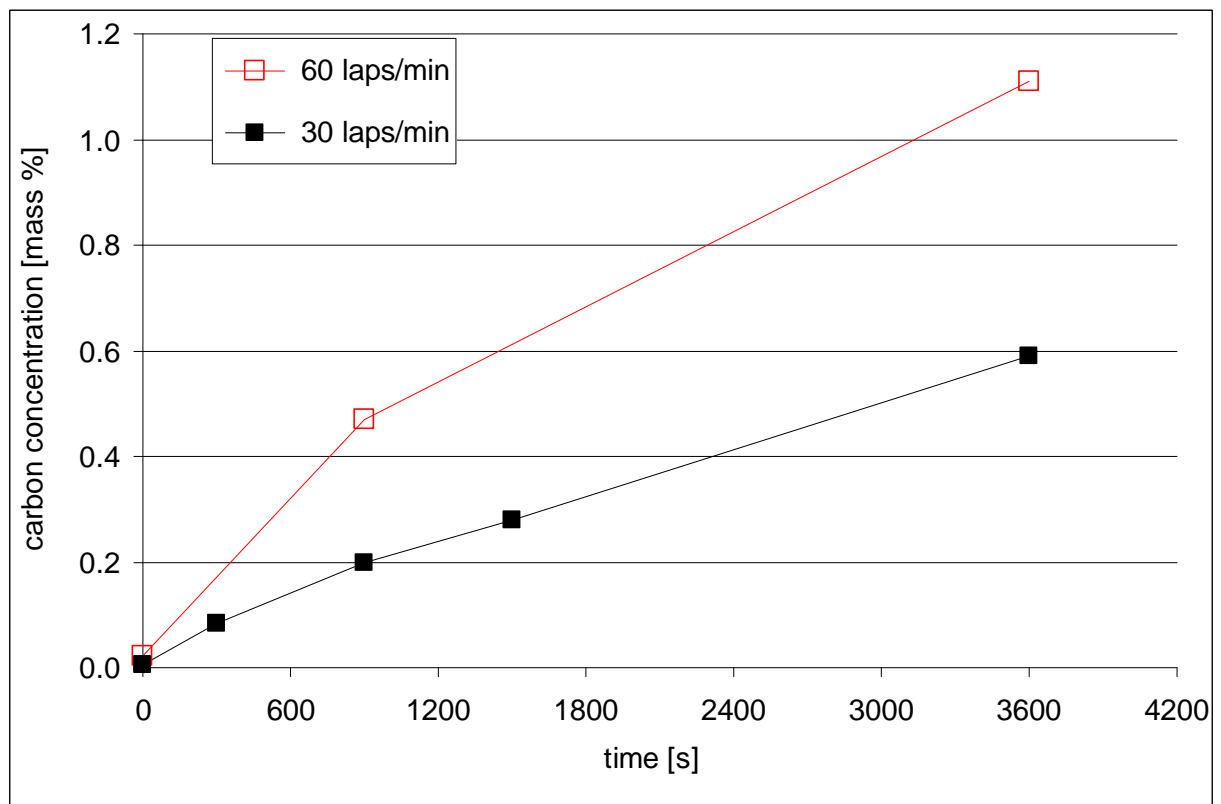**Figure 3. Comparison between of experimental and calculated mass of dissolved carbon.**

Figure 4. Experimentally measured carbon concentration in a corrosion test with zirconia graphite refractory at two different angular speeds: 30 and 60 revolutions per minute
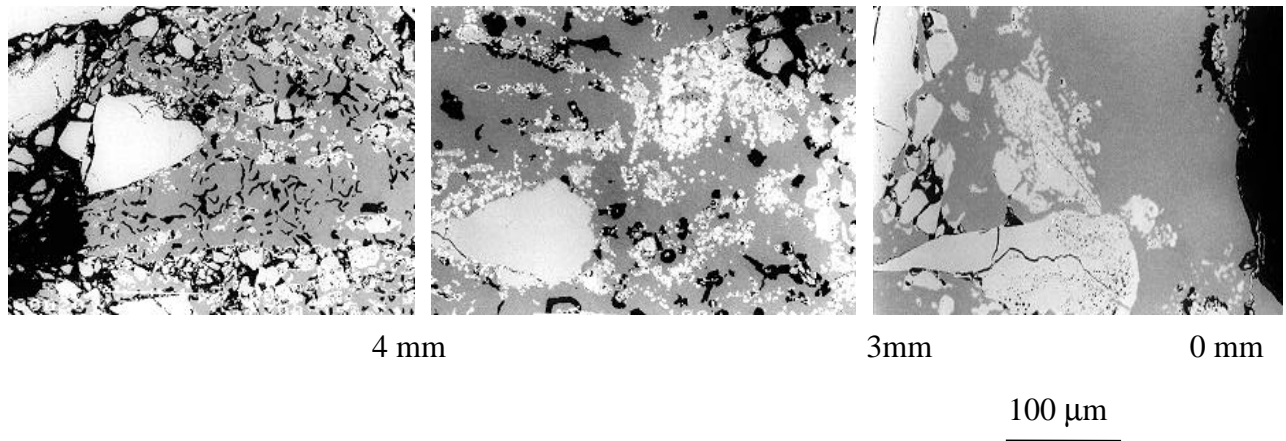
4 mm   3mm   0 mm

100 µm

Figure 5. SEM images showing steel penetrated inside ZrO$_2$-C refractory at different depth from the refractory sample surface.
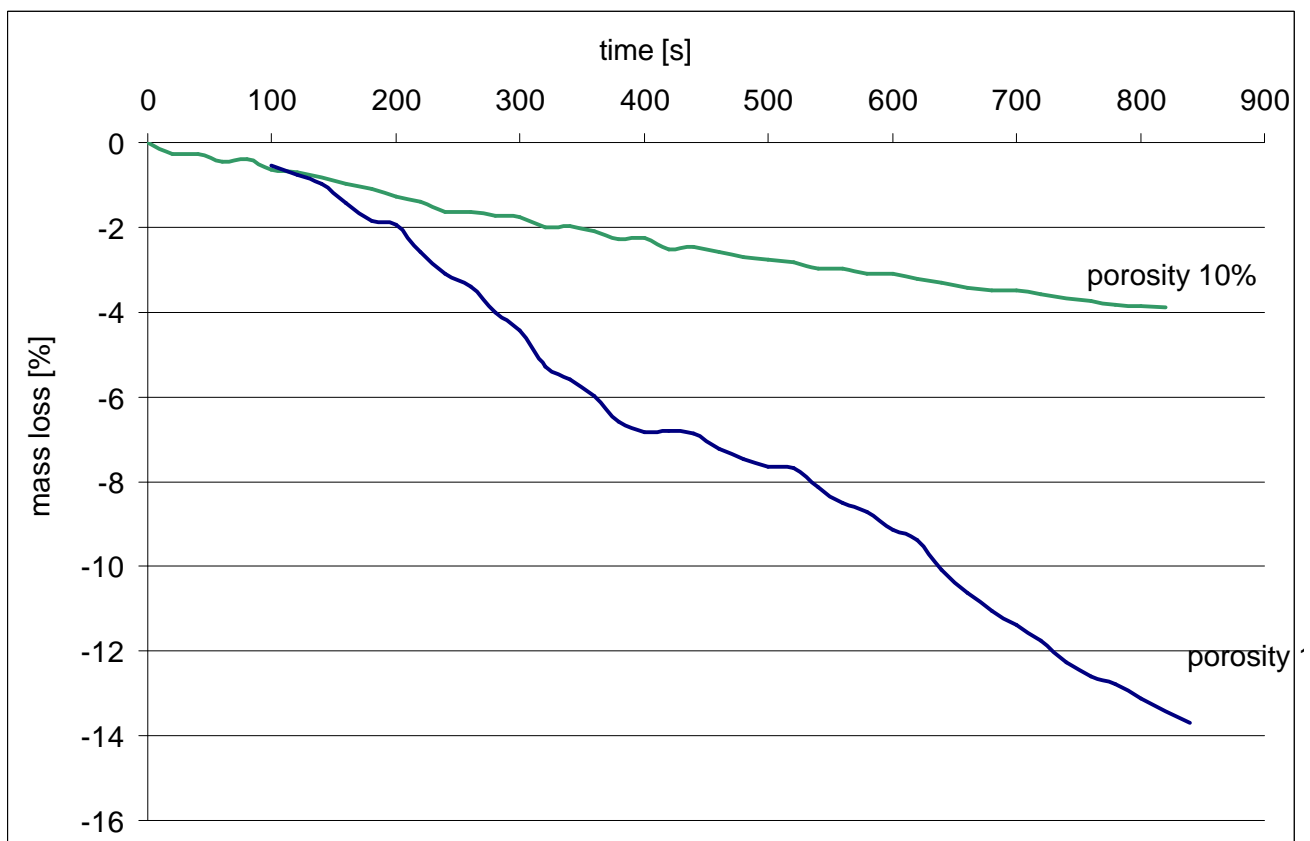
Figure 6. Mass losses of two Alumina/silica/graphite refractories purposely prepared at two different porosities. The tests were carried out at 1600°C in inert Ar atmosphere.
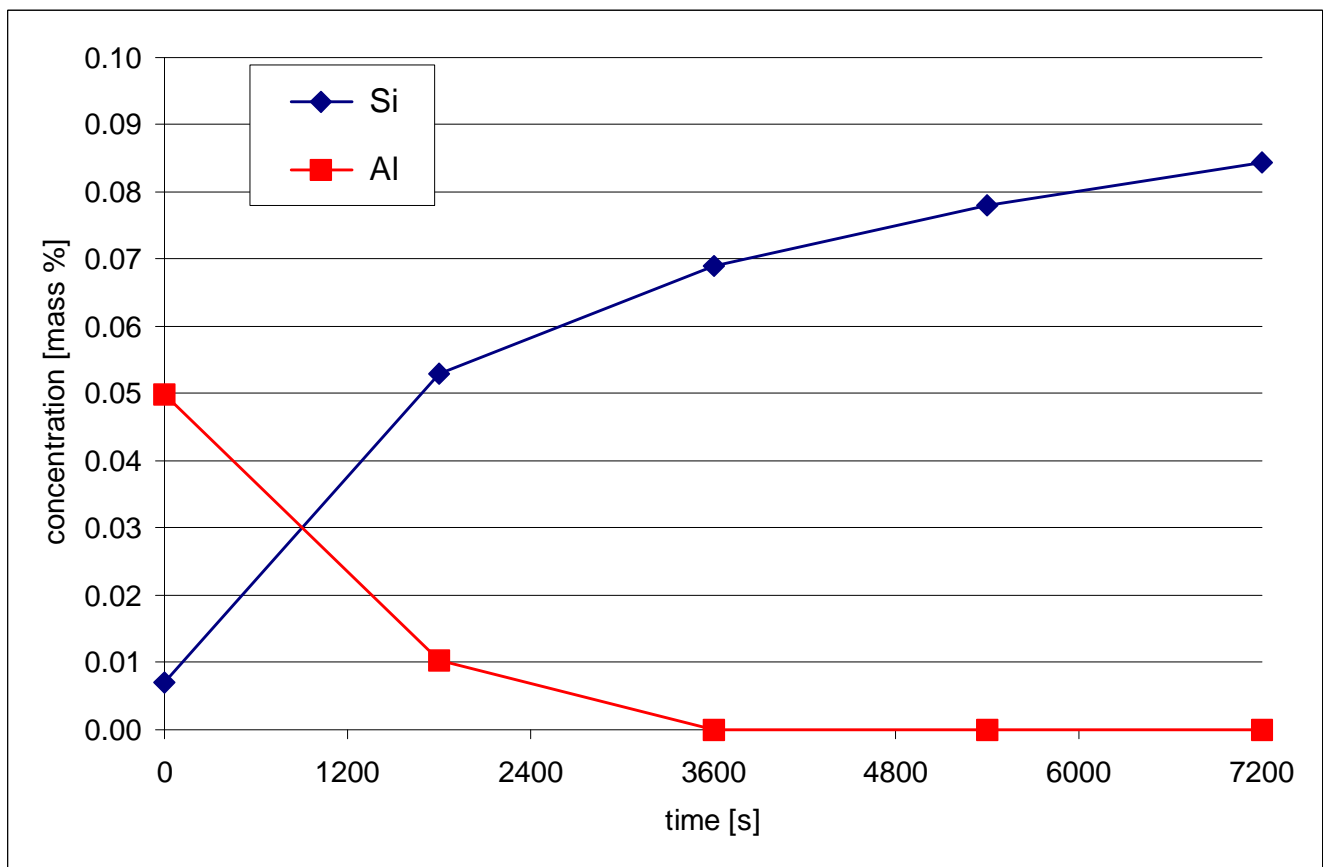
Figure 7. Concentration (mass %) of dissolved Si and Al during a corrosion test with Al$_2$O$_3$/SiO$_2$/C refractory.

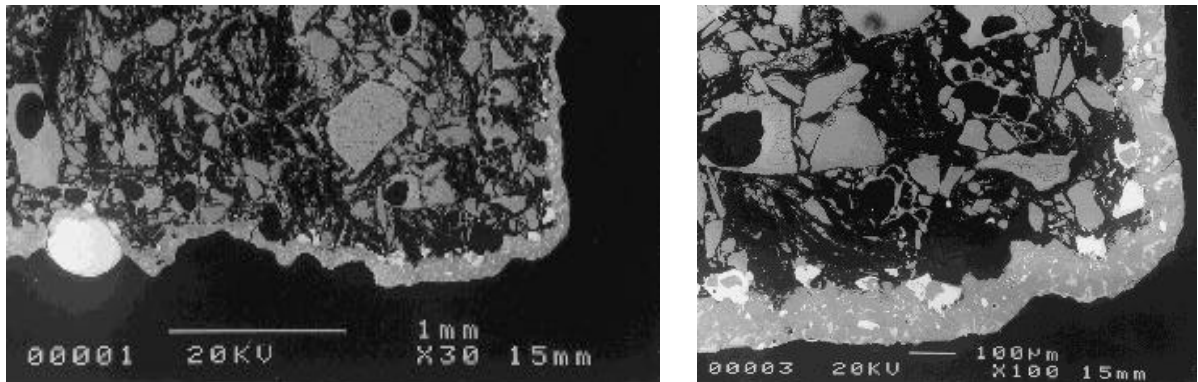**Figure 8 Interfaces formed in corrosion tests with two Al₂O₃-SiO₂-C materials.**

Matrix:

3Al₂O₃·2SiO₂

Al₂O₃ 27 %, SiO₂ 56%,

FeO 6% MnO 11%

Steel drops

Al₂O₃

10 μm
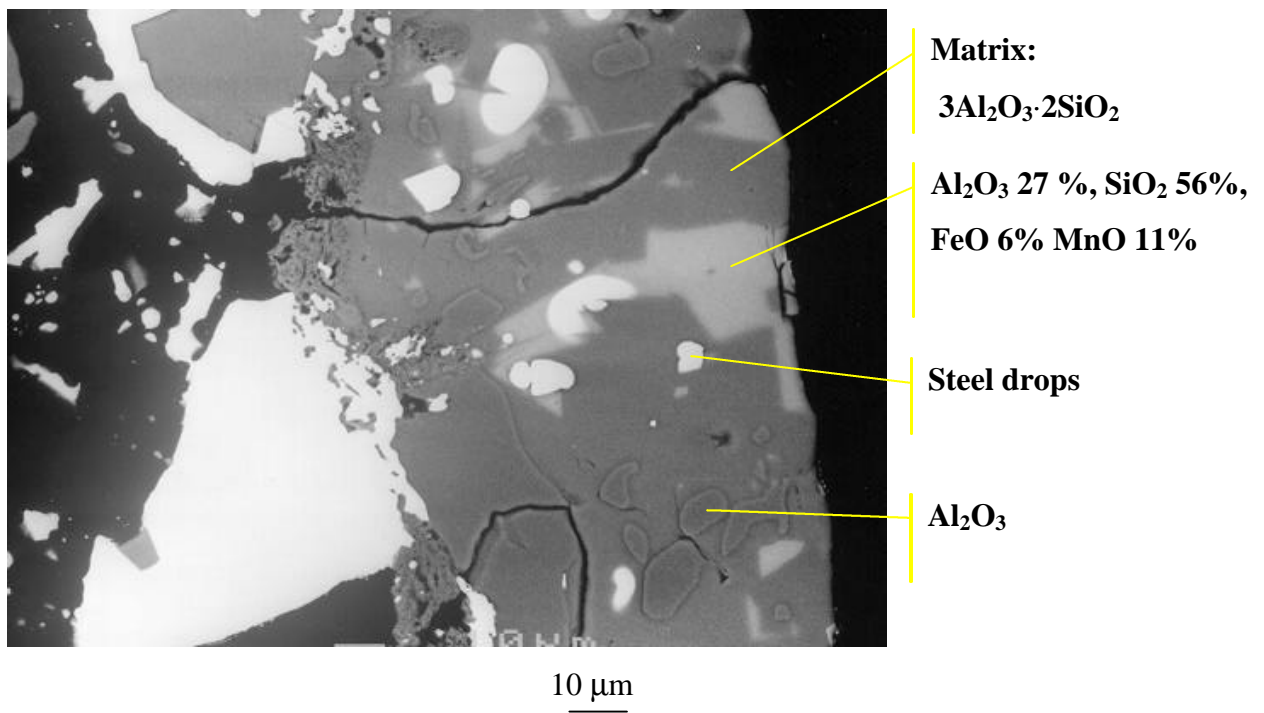
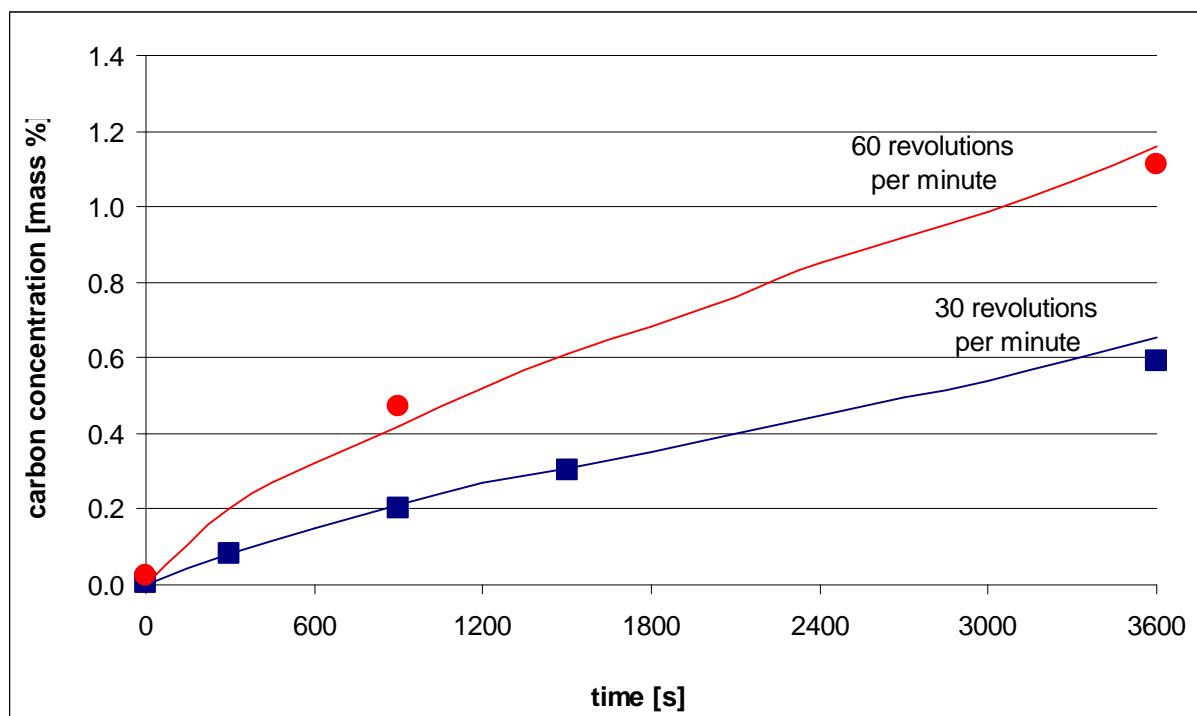**Figure 9. SEM image of the Interface zone in an Al₂O₃-SiO₂-C refractory after the corrosion test.**

Figure 10 Evolution of carbon concentration in the steel bulk calculated and measured in corrosion tests carried out using ZrO2-C material at two different rotating speeds.
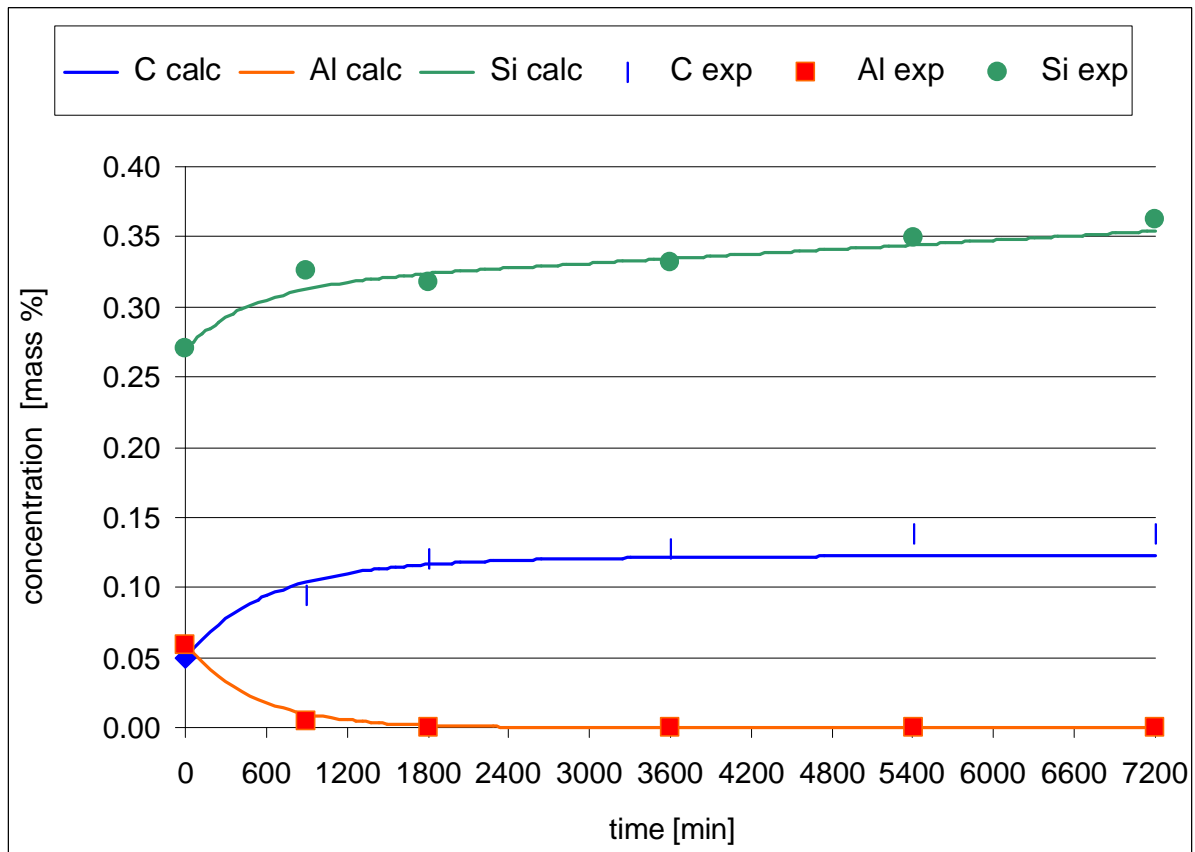
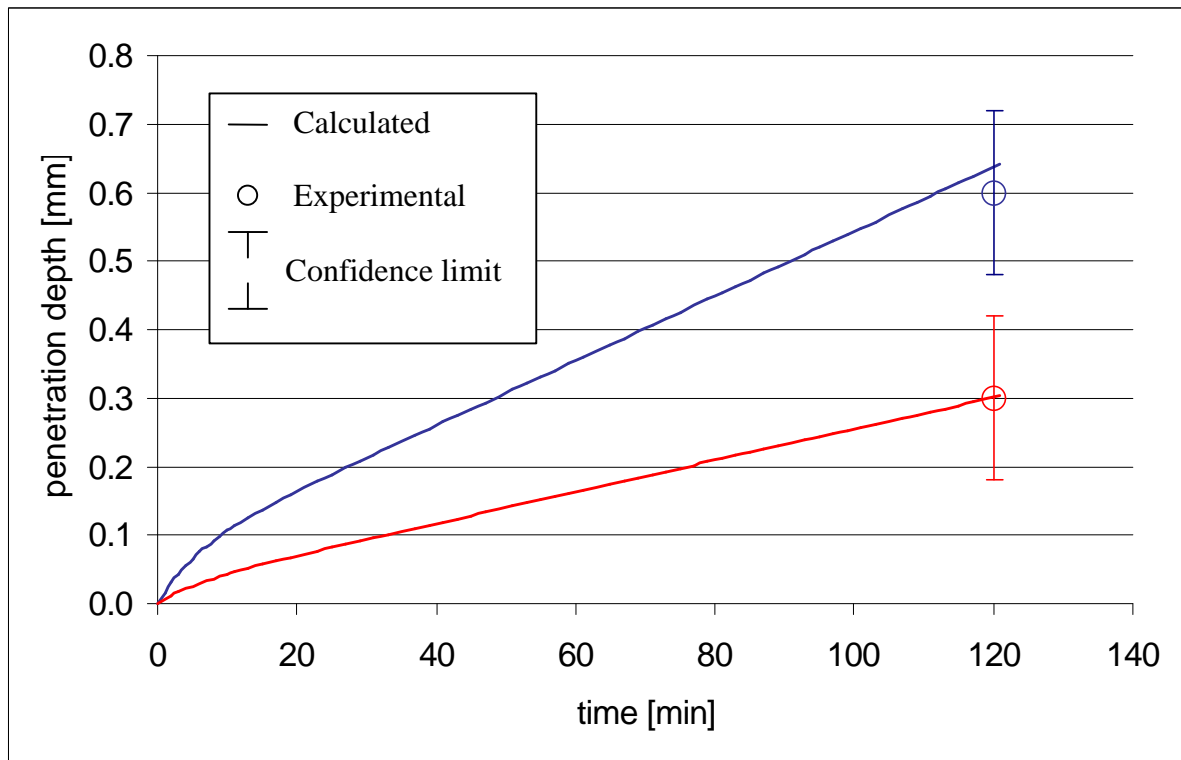**Figure 11. Steel composition calculated by the model and experimentally measured for Al$_2$O$_3$-SiO$_2$-C refractory.**

Figure 12. Steel penetration in two different Al$_2$O$_3$-C refractories with different solid carbon content.

Table 1. Main characteristics of refractory materials used in the experimentation.

Name	Refractory system	composition [mass %]	porosity [%]
M1	MgO-C	78-19	17
A1	Al_2O_3-C	83-14	17
A2	Al_2O_3-C	57-41	16
AS1	Al_2O_3-SiO_2-C	43-25-30	14
AS2	Al_2O_3-SiO_2-C	43-25-30	10
Z1	ZrO_2-C	16-77	16

Table 2. Range of chemical compositions of ideal steels used in corrosion tests

components	Pure iron [mass %]	Synthetic steel simulating ULC steel [mass %]
Al	0	0,03 – 0,05
Mn	0.05	0,3 – 0,8
Si	0.007	0,2 – 0,3
C	0.008	0,008